

Supporting Information

Fabrication of a non-semiconductor photocatalytic system using dendrite-like plasmonic CuNi bimetal combined with reduced graphene oxide nanosheet for near-infrared photocatalytic H₂ evolution

Piyong Zhang, Ting Song, Tingting Wang, Heping Zeng*

Key Laboratory of Functional Molecular Engineering of Guangdong Province, School of Chemistry and Chemical Engineering, South China University of Technology, Guangzhou, 510641, P. R. China.

*Corresponding author. Tel.: +86-20-87112631; Fax: +86-20-87112631; E-mail: hpzeng@scut.edu.cn;

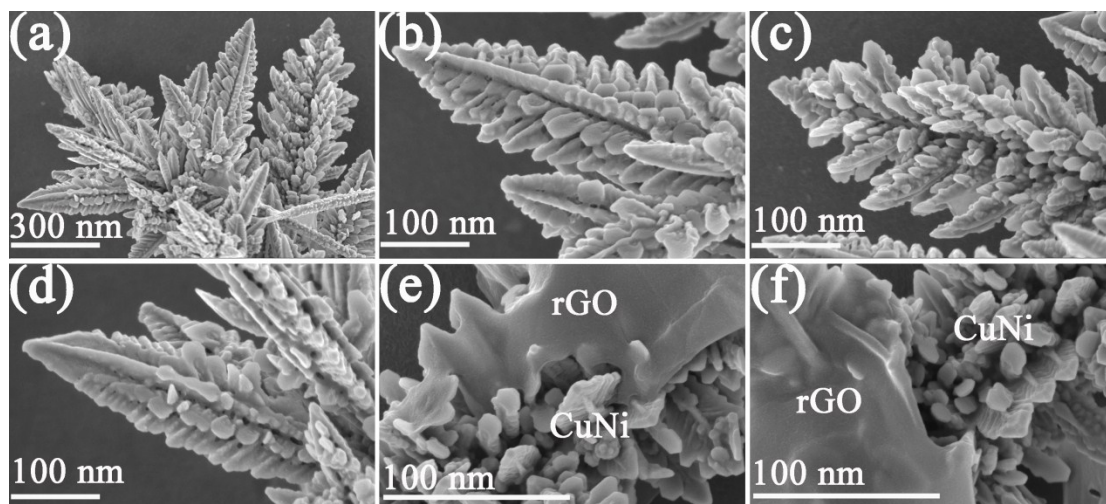


Fig. S1 (a, b, c, d) SEM images for CuNi_{5.5}, (e, f) SEM images for CuNi_{5.5}/rGO_{1wt%}.

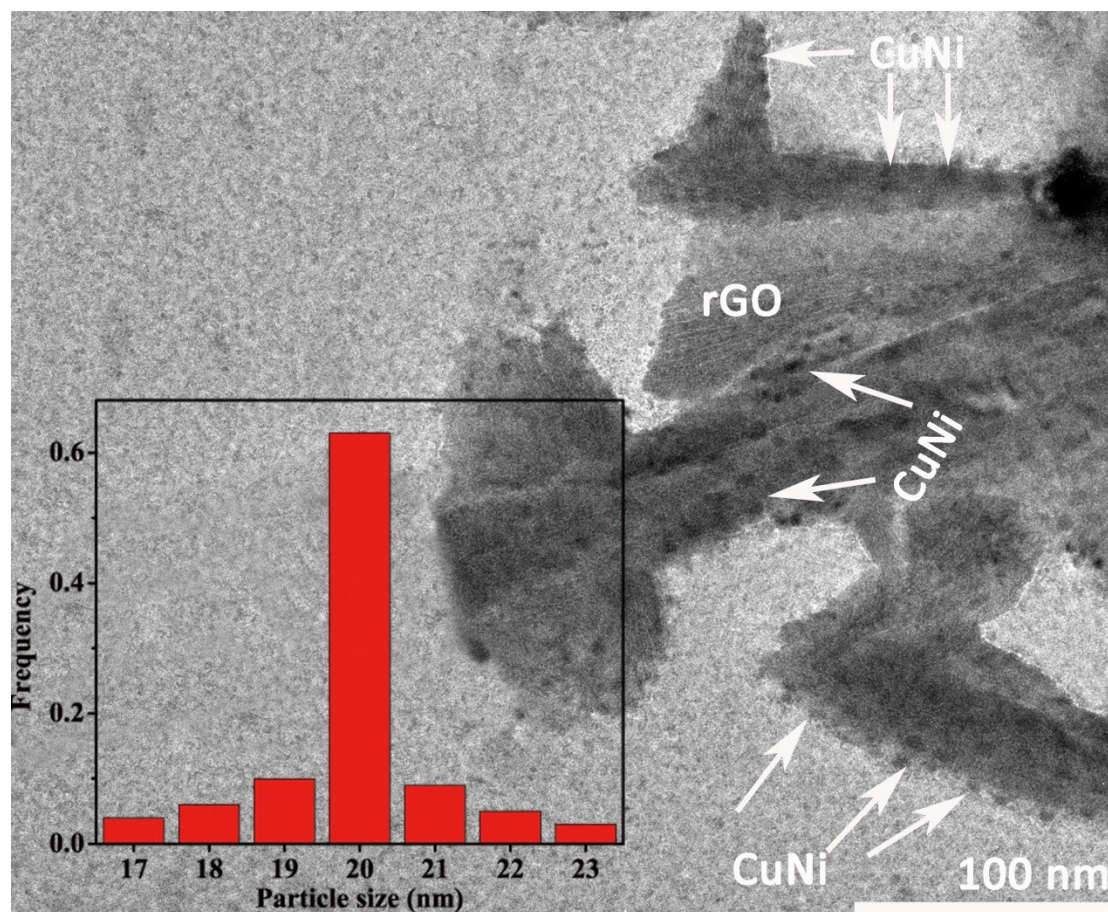


Fig. S2 Size distribution of CuNi_{5.5} bimetal.

The black points in Fig. S2 are CuNi_{5.5} bimetal and the average particle size is about 19.9 nm.

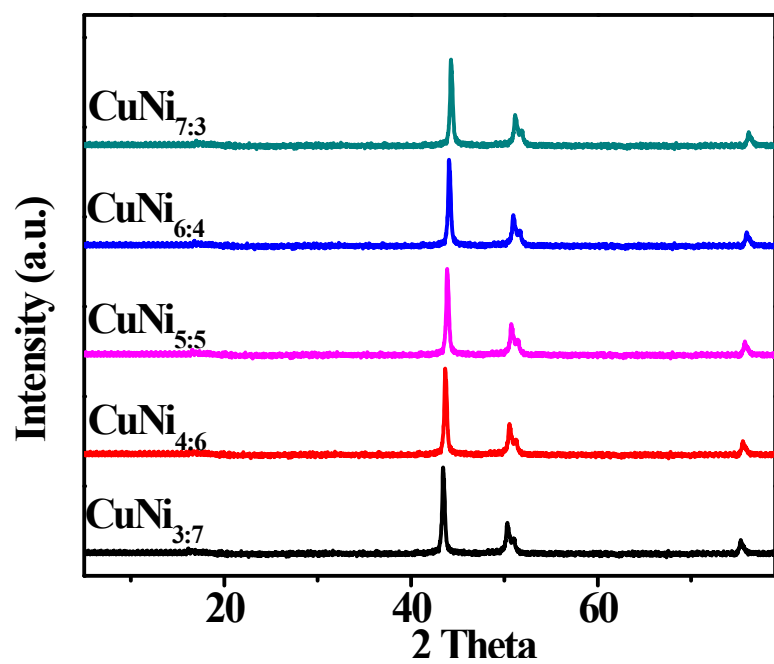


Fig. S3 XRD patterns of CuNi bimetal with different fractions.

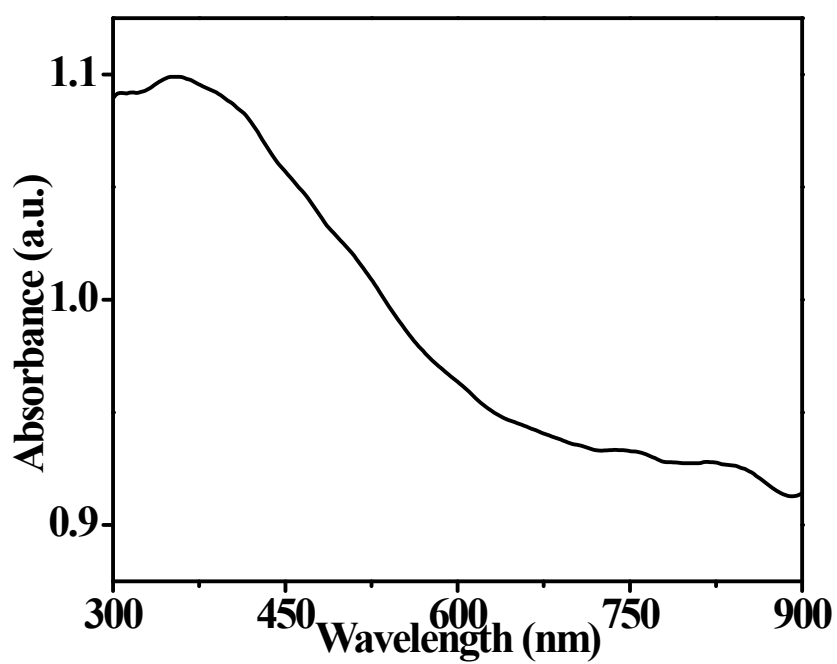


Fig. S4 UV-visible diffuse reflectance spectrum of rGO.

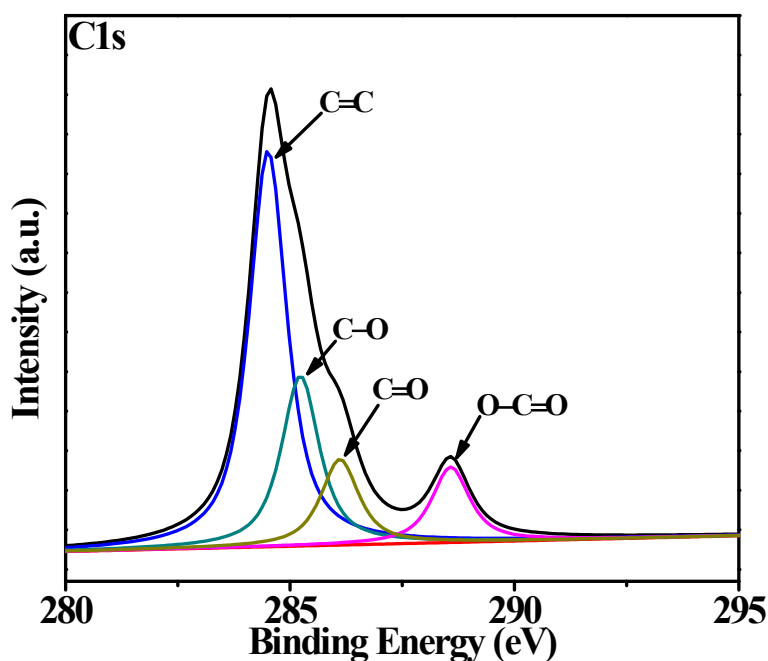


Fig. S5 C1s spectrum of GO.

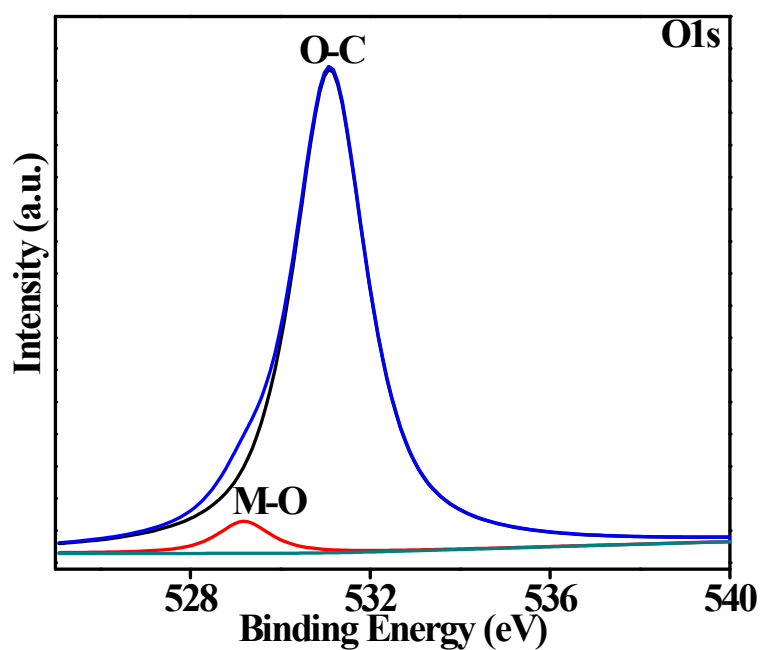


Fig. S6 O1s spectrum of CuNi_{5.5}/rGO_{1wt%}.

Fig. S6 presents the O1s spectra for the CuNi_{5.5}/rGO_{1wt%}. The asymmetric peak of the O1s spectrum indicated that there may be more than one chemical state with similar binding energy. The peaks at 529.2 eV and 531.1 eV were related to metal-oxygen (M-O) and oxygen singly bonded to carbon (C-O), respectively. This phenomenon demonstrates that chemical bond was formed between CuNi bimetal and rGO, which can promote charge transfer.

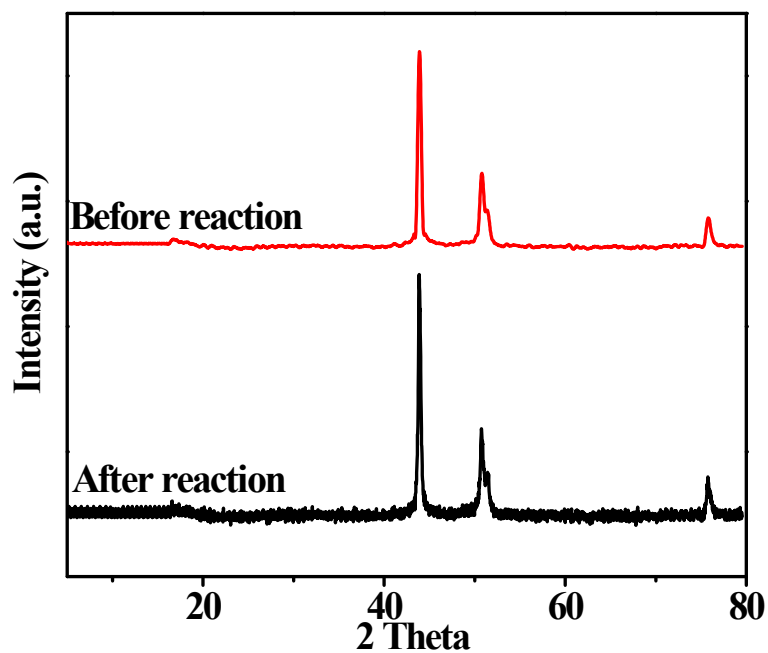


Fig. S7 XRD patterns of CuNi_{5.5}/rGO_{1wt%} before and after the stability test of hydrogen evolution.

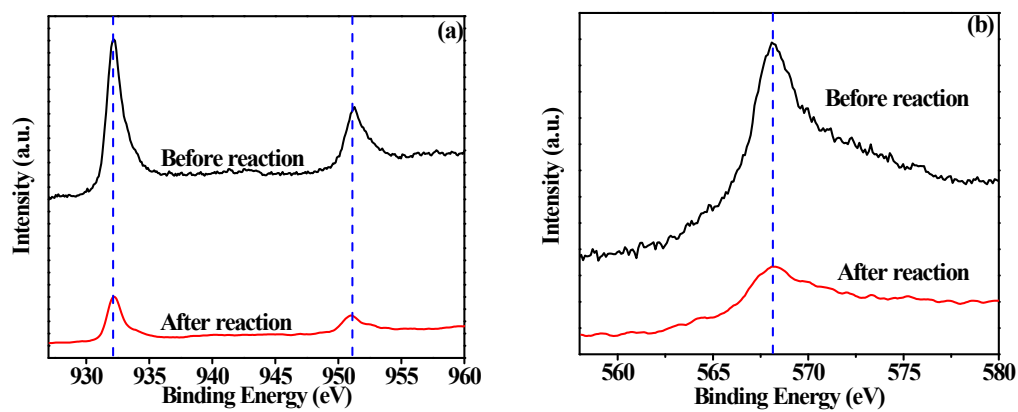


Fig. S8 XPS spectra of CuNi_{5.5}/rGO_{1wt%} before and after the stability test of hydrogen evolution, (a) Cu2p and (b) Cu LMM.

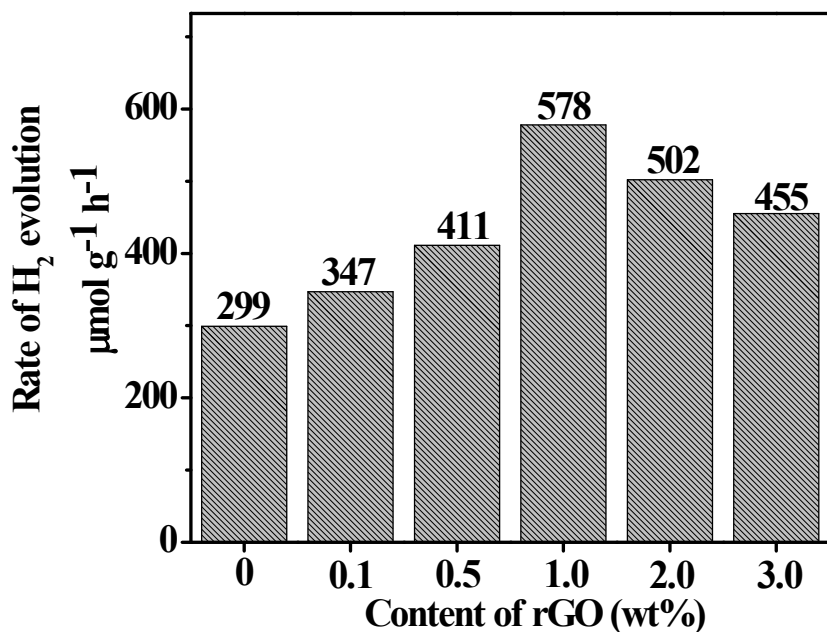


Fig. S9 Photocatalytic H₂ evolution of Cu/rGO composites.

Cu was obtained by hydrothermal method as the preparation of CuNi bimetal except the existence of Ni²⁺. Cu/rGO composites were also achieved by hydrothermal method as the preparation of CuNi/rGO photocatalyst.

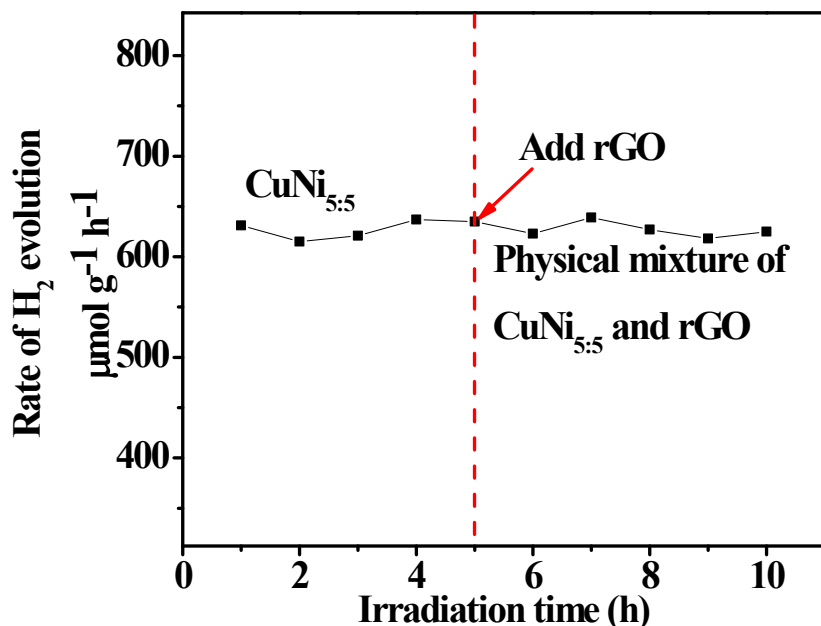


Fig. S10 Photocatalytic H₂ evolution of physical mixture between CuNi_{5.5} and rGO.

rGO was obtained by hydrothermal method as the preparation of CuNi/rGO photocatalyst except CuNi bimetal. Physical mixture of CuNi and rGO nanosheets was also investigated for photocatalytic hydrogen evolution. 60 mL deionized water,

10 mL of lactic acid and 50 mg of $\text{CuNi}_{5:5}$ were added in a 300 mL Pyrex reaction cell. The mixture solution was completely degassed about 30 minutes, followed by irradiation with a xenon lamp. H_2 evolution rate was determined using online gas chromatography every hour and this process will take about 5 hours. After 5 hour irradiation, 0.5 mg of rGO was added in above solution, followed by degassing and irradiation again. H_2 evolution rate was also determined by online gas chromatography every hour.

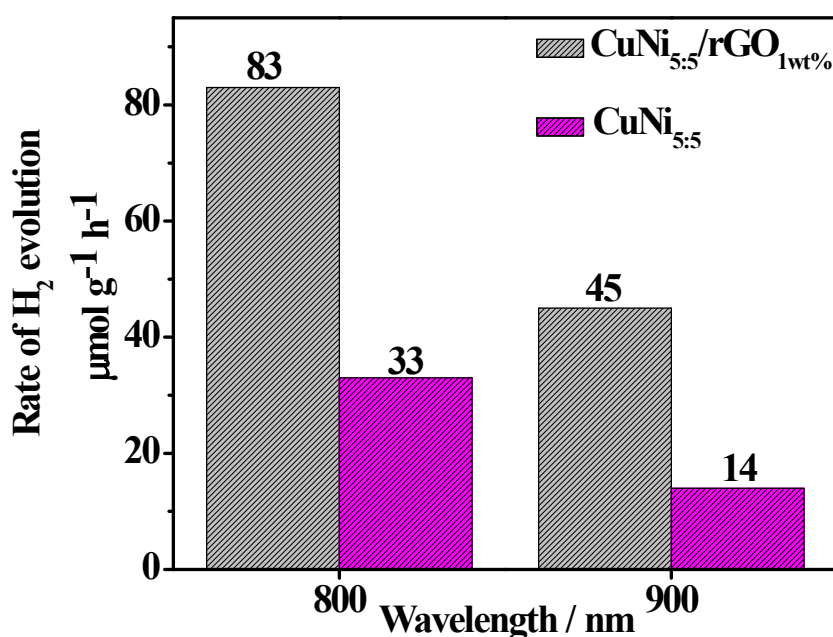


Fig. S11 Photocatalytic H_2 evolution of control experiments, reactor was wrapped by tin foil except for the light irradiation direction and the temperature was maintained at 278 K by cool following water.

Compared with Fig. 4d, there is no obvious difference on photocatalytic H_2 evolution rate, indicating that near-infrared photocatalytic H_2 evolution origin from near-infrared light excitation rather than thermal reaction or natural light excitation.

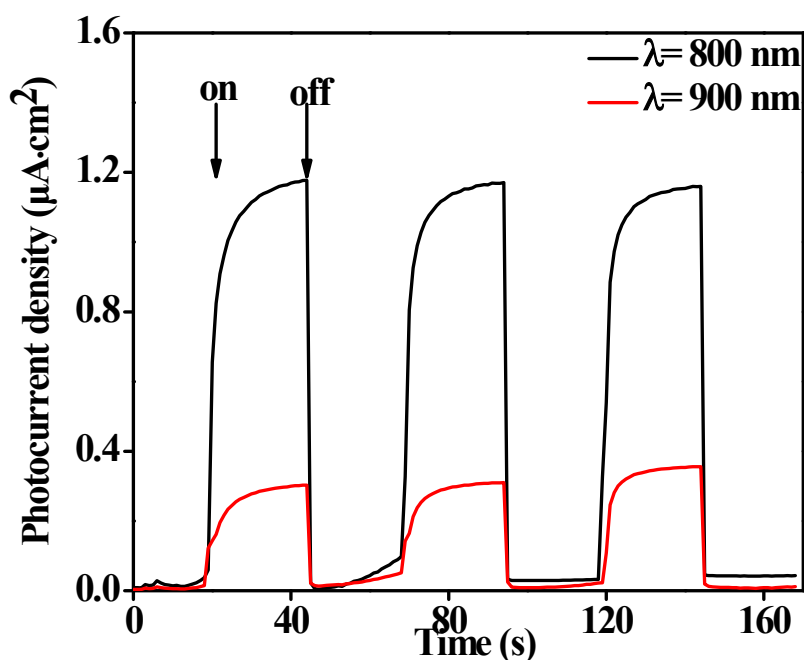


Fig. S12 Transient photocurrent density responses of CuNi_{5.5}/rGO_{1wt%} under near-infrared region.

As shown in Fig. S12, transient photocurrent responses were obtained at 800 and 900 nm irradiation, suggesting that near-infrared photocatalytic H₂ evolution origins from near-infrared light excitation. Compared with Fig. 5a, transient photocurrent values showed significant decline due to decrease of light intensity.

Table S1 BET surface area, average pore diameter and pore volume of samples.

Sample	S _{BET} (m ² g ⁻¹)	Pore Volume (cm ³ g ⁻¹)	Average pore diameter (nm)
CuNi _{5.5}	63.11	0.51	26.91
CuNi _{5.5} /rGO _{0.1wt%}	65.45	0.51	27.54
CuNi _{5.5} /rGO _{0.5wt%}	67.32	0.49	27.66
CuNi _{5.5} /rGO _{1wt%}	73.82	0.47	27.37
CuNi _{5.5} /rGO _{2wt%}	78.03	0.43	27.51
CuNi _{5.5} /rGO _{3wt%}	84.26	0.40	27.23

Table S2 Surface element composition of sample C before (1) and after (2) recycling photocatalytic reaction determined by XPS.

Sample	Elemental concentration (atom%)			
	Cu 2p	Ni 2p	C 1s	O 1s
1	7.81	7.73	69.49	14.97
2	7.32	7.11	68.55	17.02

Table S3 Quantum efficiency (QE) of CuNi_{5.5}/rGO and CuNi_{5.5} [1].

Sample	QE (800nm)%	QE (900nm)%
CuNi _{5.5}	2.50	3.31
CuNi _{5.5} /rGO _{1wt%}	6.93	9.48

The quantum efficiency is calculated from equation (1).

$$QE = \frac{2 \times \text{the number of evolved } H_2 \text{ molecules}}{\text{the number of incident photons } (N)} \times 100\% \quad (1)$$

N is determined by equation (2):

$$N = \frac{E\lambda}{hc}$$

Where E is the average intensity of irradiation which is determined by ILT 950 spectroradiometer (International Light Technologies), λ is wavelength, h is Planck constant and c is light speed.

Table S4 Photo-luminescence life time of samples.

Sample	Cu	CuNi _{5.5}	CuNi _{5.5} /rGO _{1wt%}
Life time (ns)	0.81	0.96	1.18

References

- [1] J. Liu, Y. Liu, N. Liu, Y. Han, X. Zhang, H. Huang, Y. Lifshitz, S-T Lee, J. Zhong, Z. Kang, Science, 2015, **347**, 970.